Appl Microbiol Biotechnol
DOI 10.1007/s00253-017-8525-9

Improved thermostability of a metagenomic glucose-tolerant β-glycosidase based on its X-ray crystal structure

Tomohiko Matsuzawa[1] · **Masahiro Watanabe**[2,3] · **Katsuro Yaoi**[1]

Received: 15 May 2017 / Revised: 8 August 2017 / Accepted: 7 September 2017

Abstract MeBglD2, a metagenomic β-glycosidase, is stimulated by various saccharides, including D-glucose, D-xylose, and maltose, and it promotes the enzymatic saccharification of plant biomass. To improve the thermostability of MeBglD2, its X-ray crystal structure was analyzed, and the amino acid residues responsible for its thermostability were identified using the structural information. Mutations in His8, Asn59, and Gly295 improved the thermostability of MeBglD2, and the combination of these mutations resulted in the highest thermostability. Compared with wild-type MeBglD2, thermostable MeBglD2 mutants promoted plant biomass saccharification using *Trichoderma reesei* cellulase. In addition to thermostability, the thermostable mutants exhibited higher tolerance to ethanol, dimethyl sulfoxide, and copper ions, indicating that the MeBglD2 mutants generated in this study were improved in their tolerance to not only high temperature but also to organic solvents and metal ions.

Keywords β-glycosidase · Metagenome · Biomass · Thermostabilization

Tomohiko Matsuzawa and Masahiro Watanabe contributed equally to this work.

Electronic supplementary material The online version of this article (https://doi.org/10.1007/s00253-017-8525-9) contains supplementary material, which is available to authorized users.

✉ Tomohiko Matsuzawa
matsuzawa-tomohiko@aist.go.jp

✉ Katsuro Yaoi
k-yaoi@aiat.go.jp

[1] Bioproduction Research Institute, National Institute of Advanced Industrial Science and Technology (AIST), Tsukuba Central 6, 1-1-1 Higashi, Tsukuba, Ibaraki 305-8566, Japan

[2] Biomass Refinery Research Center, National Institute of Advanced Industrial Science and Technology (AIST), 3-11-32, Kagamiyama, Higashi-Hiroshima, Hiroshima 739-0046, Japan

[3] Research Institute for Sustainable Chemistry, National Institute of Advanced Industrial Science and Technology (AIST), 3-11-32, Kagamiyama, Higashi-Hiroshima, Hiroshima 739-0046, Japan

Introduction

β-Glucosidases, β-D-glucoside hydrolases (EC 3.2.1.21), are widely distributed and vital for many enzymatic processes, including plant biomass saccharification (Nakazawa et al. 2012; Baba et al. 2015; Uchiyama et al. 2015; Del Pozo et al. 2012). In plant biomass saccharification, β-glucosidases hydrolyze cellooligosaccharides, such as cellobiose and cellotriose, into D-glucose. Cellooligosaccharides are produced during cellulose degradation by cellulases, such as cellobiohydrolases (Nummi et al. 1983; Teeri et al. 1998) and endo-glucanases (Saloheimo et al. 1988; Biely et al. 1991). Because cellooligosaccharides inhibit the activities of cellulases (Murphy et al. 2013), β-glucosidases play a vital role in plant biomass saccharification. However, most β-glucosidases are also inhibited by their reaction product, D-glucose (i.e., product inhibition) (Xiao et al. 2004). Product inhibition of β-glucosidases is one of the major bottlenecks of plant biomass saccharification because the inhibition of β-glucosidase will eventually lead to the accumulation of cellooligosaccharides and the inhibition of cellulases (Teugjas and Väljamäe 2013). Several glucose-tolerant β-glucosidases have been isolated and characterized (Jabbour et al. 2012; Uchima et al. 2012; Uchiyama et al. 2013; Ramani et al. 2015; Yang et al. 2015; Matsuzawa et al. 2016a). A β-glycosidase termed MeBglD2, which not only exhibits β-glucosidase activity but also β-galactosidase and β-fucosidase activities, was isolated from the soil metagenome

Published online: 23 October 2017

(Matsuzawa and Yaoi 2017). The β-glucosidase and β-fucosidase activities of MeBglD2 are stimulated by many types of saccharides, such as D-glucose, D-xylose, D-galactose, cellobiose, and maltose. For example, the *p*-nitrophenol (*p*NP) release activity toward *p*NP β-D-glucopyranoside, which may include hydrolytic and transglycosylation activities, is activated approximately 3.6-, 3.9-, and 6.3-fold by adding 50 mM D-glucose, D-xylose, and maltose, respectively. MeBglD2 promotes plant biomass saccharification using *Trichoderma reesei* cellulase (including endo-glucanase, cellobiohydrolase, β-glucosidase, endo-xylanase, etc.) by degrading cellooligosaccharides, such as cellobiose and cellopentaose (Matsuzawa and Yaoi 2017).

The thermostability of an enzyme is highly significant for its industrial utilization. Several thermostable β-glycosidases have been isolated from thermophilic bacteria (Dion et al. 1999; Liebl et al. 1994; Yernool et al. 2000). In contrast, although MeBglD2 exhibits many unique and beneficial properties, as described above, the thermostability of MeBglD2 is much lower than those of the β-glycosidases of thermophilic bacteria. In this study, the crystal structure of MeBglD2 was solved, and the three-dimensional structure and amino acid sequence of MeBglD2 were compared with those of thermostable β-glycosidases isolated form thermophilic bacteria. The amino acid residues responsible for the thermostability of MeBglD2 were also predicted. Using site-directed mutagenesis, we successfully generated thermostable MeBglD2 mutants that improved plant biomass saccharification.

Materials and methods

Materials

Chromogenic substrates were obtained as described previously (Matsuzawa and Yaoi 2017), and alkaline-pretreated rice straw was prepared as described previously (Matsuzawa et al. 2015).

Site-directed mutagenesis

The primers used for site-directed mutagenesis are listed in Table S1 (see Supplemental Materials). Primer pairs 1 and 2, 1 and 3, and 1 and 4 were used for mutation of site I (Fig. 1 and Table S2 in the Supplemental Materials). Primer pairs 5 and 6, 7 and 8, 9 and 10, 11 and 12, 13 and 14, 15 and 16, 17 and 18, 19 and 20, and 21 and 22 were used for mutation of sites II, III, IV, V, VI, VII, VIII, and IX, respectively (Fig. 1). Primer pairs 23 and 24 and 23 and 25 were used for mutation of site X (Fig. 1 and Table S2). DNA fragments were amplified by polymerase chain reaction (PCR) using PrimeStar Max DNA Polymerase (Takara Bio, Shiga, Japan), the primer pairs described above, and pET28a-MeBglD2 as the template (Matsuzawa and Yaoi 2017). The PCR products were treated with *Dpn*I to remove the template, ligated using the In-Fusion HD Cloning Kit (Takara Bio), and introduced into *Escherichia coli* BL21 (DE3) cells (Nippon Gene, Tokyo, Japan).

Expression and purification of MeBglD2 mutants

E. coli BL21 (DE3) cells harboring pET28a-MeBglD2 mutants were cultured on Overnight Express Instant LB Medium (Novagen, Madison, WI, USA) containing 20 μg/ml kanamycin at 25 °C for 24 h. Cells were collected by centrifugation (5000*g* at 4 °C for 5 min) and resuspended in BugBuster (Novagen) containing 0.024 units/ml Benzonase (Novagen) and cOmplete™ EDTA-FREE protease inhibitor cocktail (Roche, Basel, Switzerland). After incubation at room temperature for 30 min, cell debris was removed by centrifugation (13,000*g* at 4 °C for 10 min) and filtration (0.45 μm). Wild-type and mutant MeBglD2 enzymes were purified using a nickel affinity column (HisTrap HP, GE Healthcare, Buckinghamshire, England) and used for crystal structure analysis and determinations of thermostability and optimal temperature. Partial purification of the mutant enzymes was performed using His SpinTrap columns (GE Healthcare), which were then used to screen for thermostable mutants.

Crystallization and X-ray data collection

The purified enzymes were dialyzed against 20 mM Tris-HCl (pH 8.0)/50 mM NaCl and concentrated to 7 mg/ml using Vivaspin 20-10K centrifugal filter units (GE Healthcare). The initial crystallization screening of MeBglD2 was performed using Crystal Screen HT (Hampton Research, Aliso Viejo, CA, USA) at 20 °C by the sitting-drop vapor diffusion method, in which a 0.5-μl volume of protein solution was mixed with an equal volume of reservoir solution. Small crystals were grown for 1 week in reagent no. H5 (0.1 M Tris-HCl buffer (pH 8.5), 1.0 M lithium sulfate, and 0.01 M nickel chloride). The crystallization conditions were further optimized using the hanging-drop vapor diffusion method, in which a 2-μl volume of protein solution was mixed with an equal volume of reservoir solution. The optimal crystals were grown in 0.1 M Tris-HCl buffer (pH 8.5), 1.1–1.3 M lithium sulfate, and 0.01 M nickel chloride for 2 weeks at 20 °C. The resulting crystals were then soaked in reservoir solution containing 30% (*v*/*v*) glycerol as a cryoprotectant. X-ray data were collected at the SPring-8 BL44XU (Hyogo, Japan). The dataset was collected at a single wavelength of 0.9 Å using the Rayonix MX300HE detector. The crystal was rotated 200° with an oscillation angle of 0.5° per frame (total of 400 frames). The distance from the crystal to the detector was 250 mm. All data were processed using the HKL2000 software package (DENZO and SCALEPACK) (Otwinowski and Minor 1997).

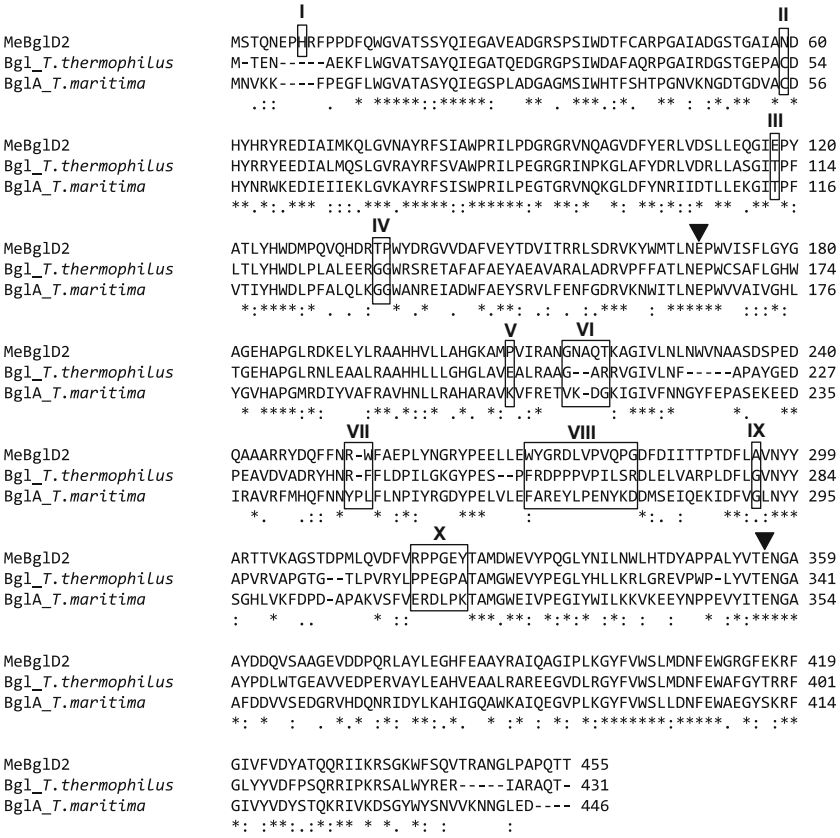

Fig. 1 Amino acid sequence alignment of β-glycosidase, metagenomic MeBglD2, *T. thermophilus* Bgl, and *T. maritima* BglA. Sequence alignment was performed using the ClustalW program (http://clustalw.ddbj.nig.ac.jp/) with the default settings. Asterisks indicate positions that are fully conserved residues. Colons and periods indicate conservation between groups of strongly and weakly similar properties, respectively. Black triangles indicate the two catalytic glutamate residues. The mutated sites are indicated

Structural analysis

General data handling was carried out using the CCP4 package (Collaborative Computational Project, Number 4, 1994). The initial model of MeBglD2 was solved by PHASER (McCoy et al. 2007), with a search model of β-glucosidase B from *Bacillus polymyxa* (Protein Data Bank [PDB] code 2jie). The model was built, and water molecules were added using ARP/wARP (Langer et al. 2008). Refinements were carried out using REFMAC5 (Murshudov et al. 2011). Further refinement was performed using COOT (Emsley and Cowtan 2004), and model geometry was analyzed using RAMPAGE (Lovell et al. 2003). Figures were created using CCP4MG (Potterton et al. 2004).

Differential scanning fluorimetry

Differential scanning fluorimetry (DSF) experiments were carried out on the CFX96 Real-Time PCR System™ (Bio-Rad, Hercules, CA, USA) using 450/490 excitation and 560/580 emission filters in a 96-well plate format (Watanabe et al. 2014). Each enzyme was prepared at a final concentration of 1.0 mg/ml in 50 mM sodium acetate buffer (pH 5.0). SYPRO orange dye (5000-fold stock solution in dimethyl sulfoxide (DMSO); Invitrogen, Carlsbad, CA, USA) was added to the enzyme (1:20 dilution; Senisterra and Finerty 2009). The negative control comprised buffer and the SYPRO mixture without MeBglD2. Each sample (20 μl per well) was measured from 25 to 90 °C using a stepwise gradient of 0.5 °C per 5 s. Following curve fitting of the data to the Boltzmann equation, the melting temperature (T_m) of each enzyme was calculated using Bio-Rad CFX Manager software (Bio-Rad).

The thermostability and optimal temperature of MeBglD2 mutants

The thermostability of each MeBglD2 mutant was examined as described below. In brief, 10 μl enzyme solution containing 160 mM sodium phosphate buffer (pH 6.0) and 0.1 μg enzyme was incubated at 50–68°C for 30 min. Next, 10 μl 10 mM *p*NP β-D-glucopyranoside was added as a substrate and incubated at 60 °C for 5 min. To terminate the reaction, 50 μl 1 M $NaHCO_3$ were added. The concentration of released *p*NP was determined by measuring the absorbance at 405 nm.

The optimal temperature of each mutant enzyme was determined as described below. Briefly, 20-μl reaction mixtures containing 80 mM sodium phosphate buffer (pH 6.0), 0.04 μg purified enzyme, and 5 mM *p*NP β-D-glucopyranoside were incubated at 55–77.5 °C for 5 min. After addition of 50 μl 1 M $NaHCO_3$, the concentration of released *p*NP was measured as described above.

Substrate specificities of the MeBglD2 mutants

The hydrolytic activity of the MeBglD2 mutants toward chromogenic substrates (*p*NP β-D-glucopyranoside, *p*NP β-D-galactopyranoside, and *p*NP β-D-fucopyranoside) was evaluated as described previously (Matsuzawa and Yaoi 2017). The hydrolytic activity of MeBglD2 and variants thereof toward cellobiose was evaluated as described below. Reaction mixtures of 20 μl containing 5 mM cellobiose, 50 mM sodium phosphate buffer (pH 6.0), and 0.05 μg purified enzyme were incubated at 40 °C for 5 min. To inactivate the enzyme, the reaction mixture was incubated at 98 °C for 10 min. Glucose was measured using a LabAssay™ Glucose Kit (Wako Pure Chemical Industries, Osaka, Japan). Because the hydrolysis of one molecule of cellobiose produces two molecules of D-glucose, absorbance values were divided by two. The experiment was performed in triplicate.

Biomass saccharification

The enzymatic saccharification of pretreated plant biomass using *T. reesei* (PC-3-7 strain) cellulase and purified enzyme was performed as described previously (Matsuzawa and Yaoi 2017), with slight modifications. In brief, 2-ml reaction mixtures containing 538 mg alkaline-pretreated rice straw (water content 81.4%) (Matsuzawa et al. 2015), 100 mM sodium phosphate buffer (pH 6.0), 200 μg *T. reesei* cellulase, and 40 μg purified MeBglD2 mutants were incubated at 40 °C for 24–72 h with weak agitation (150 rpm). To inactivate the enzymes, supernatants were incubated at 100 °C for 5 min, and the sugars produced were measured using the 3,5-dinitrosalicylic acid reagent method (Miller 1959).

Effects of organic solvents and copper ions on MeBglD2 mutants

The effects of organic solvents (ethanol and DMSO) and copper ions on the β-glucosidase activities of the MeBglD2 mutants were examined as described below. Briefly, 20-μl reaction mixtures containing 100 mM sodium phosphate buffer (pH 6.0), 0.05 μg purified enzyme, 5 mM *p*NP β-D-glucopyranoside, and additives (10% (*v*/*v*) ethanol, 10% (*v*/*v*) DMSO, or 5 mM $CuSO_4$) were incubated at 60 °C for 5 min. To terminate the reaction, 50 μl of 1 M $NaHCO_3$ were added, and the concentration of the released *p*NP was measured as described above.

PDB accession number

The coordinates and structural factors for MeBglD2 were deposited in the Protein Data Bank (PDB) under accession number 5XGZ.

Results

Comparison of MeBglD2 and thermostable β-glycosidase amino acid sequences

To improve the thermostability of the metagenomic β-glycosidase MeBglD2, the amino acid sequence of MeBglD2 was compared with those of thermostable β-glycosidases isolated from the thermophilic bacteria *Thermus thermophilus* (Dion et al. 1999) and *Thermotoga maritima* (Liebl et al. 1994) (Fig. 1). The MeBglD2 sequence was similar to those of *T. thermophilus* Bgl (UniProtKB accession no. Q53W75, identity 52%) and *T. maritima* BglA (UniProtKB accession no. Q08638, identity 50%). Because there were many amino acid differences between the sequences of MeBglD2 and other thermostable β-glycosidases (Fig. 1), we could not identify the amino acid residues responsible for the thermostability of MeBglD2 by comparison of amino acid sequences. To identify the amino acid residues responsible for the thermostability of MeBglD2, the crystal structure of MeBglD2 was analyzed and compared with those of thermostable β-glycosidases from *T. thermophilus* and *T. maritima*.

Overall structure of MeBglD2

The prepared crystals belonged to space group *I*23, unit cell a = b = c = 202.4 Å. The asymmetric unit consisted of two molecules with a solvent content of 64.4%, which corresponded to a Matthews coefficient of 3.46 $Å^3$ Da^{-1} (Matthews 1968). After refinement, R_{work} was estimated at 19.5% and R_{free} at 25.5%. Data collection and refinement statistics are shown in Table 1. The overall structure of MeBglD2, constructed from Glu6 to Pro450, was determined at 1.75 Å. The structure of MeBglD2 consisted of a traditional TIM-barrel fold $(\beta/\alpha)_8$ and several external α-helices and β-barrels (Fig. 2a). A Dali search for structural similarity to MeBglD2 revealed other β-glycosidases belonging to the glycoside hydrolase family 1, such as BglA from *T. maritima* (*Z*-score of 63.0 and root-mean-square deviation (RMSD) of 1.1 Å over 433 Cα atoms) (PDB 1OD0) (Zechel et al. 2003) and Bgl from *T. thermophilus* HB8 (*Z*-score of 62.2 and RMSD of 1.2 Å over 423 Cα atoms) (PDB 4BCE) (Teze et al. 2014). Based on the superimposed structure and the amino acid sequence alignment (Fig. 1) of the three enzymes, we hypothesized that the putative active residues of MeBglD2 consist of a nucleophilic Glu356 and an acid/base Glu170. Moreover, the two catalytic residues, located at the traditional cleft structure of the GH1 family, were bound to three glycerol molecules (Fig. 2b). Two nickel ions were bound to His64 NE2 and Arg197 NH1, and one sulfide ion was bound to His345 NE2.

Table 1 Data collection and refinement statistics of the MeBglD2 crystal structure

Data collection	
Wavelength (Å)	0.9
Space group	*I*23
Unit cell (a, b, c (Å))	202.4, 202.4, 202.4
(α, β, γ (°))	90, 90, 90
Resolution range (Å)	50.0–1.75 (1.78–1.75)[a]
Total no. of reflections	1,142,725
No. of unique reflections	134,784
Redundancy	8.5 (3.2)[a]
Completeness (%)	98.0 (93.3)[a]
R_{merge} (%)[b]	7.2 (64.8)[a]
$< I/\sigma(I) >$	11.9 (2.1)[a]
Refinement	
Resolution range (Å)	30.0–1.75
R_{work} (%)[c]/R_{free} (%)[d]	20.6/25.5
No. of atoms	
Protein	7270
Ligand	104
Water	510
R.M.S. deviations	
Bond lengths (Å)	0.020
Bond angles (°)	1.8
Average *B*-factor (Å^2)	20.8
Ramachandran statistics (%)	
Favored region	96.8
Allowed region	2.9
PDB accession number	5XGZ

[a] Outer shell (1.78–1.75 Å)

[b] $R_{merge} = \sum_{hkl}\sum_i |I_i(hkl) - \langle I(hkl)\rangle| / \sum_{hkl}\sum_i Ii(hkl)$, where I_i(hkl) is the scaled intensity of the *i*th observation of reflection *hkl*. $\langle I(hkl)\rangle$ is the mean value and the summation is over all measurements

[c] $R_{work} = \sum_h \sum_i ||F_o|-|F_c||/\sum|F_o|$

[d] R_{free} is R_{work} for approximately 5% of the reflections that were excluded from the refinement

To improve the thermostability of MeBglD2, we first carefully generated ten mutations using site-directed mutagenesis (H8L, H8I, H8V, N59C, E118T, 136GG, P210K, 254P, 253GPL, and A295G) and four cassette mutations (216Tm, 271Tm, 319Tm, and 319Tt) (Table S2) based on the crystal structures and amino acid sequences of MeBglD2 and two thermostable enzymes, *T. maritima* BglA and *T. thermophilus* Bgl (Figs. 1 and 3a). Because the N- and C-termini of MeBglD2 are located in close proximity, His8 was replaced with hydrophobic residues (i.e., leucine, isoleucine, or valine) to form a hydrophobic bond between the N- and C-termini (Figs. 2a and 3a). In the N59C mutant, the hydroxyl group (OD1) of Asn59 was spatially close to the side chain (CE) of Met406 (length 3.45 Å) (Fig. 3b). If asparagine is replaced with another hydrophobic residue, such as leucine, isoleucine, or cysteine (except for aromatic amino acids), it may form a new hydrophobic contact with Met406 in MeBglD2. Moreover, the Asn59 in BglA and Bgl was replaced with a hydrophobic residue, cysteine. In the A295G mutant, because the glycine residues at site IX (Fig. 1) were well conserved in both BglA and Bgl, Ala295 of MeBglD2 was replaced with a glycine residue. Other mutation sites were selected to correspond to at least one of the following three rules: (1) amino acid residues that are well conserved in *T. maritima* BglA and *T. thermophilus* Bgl, but not in MeBglD2; (2) amino acid residues that appear to have no effect on catalytic activity (e.g., those located close to the catalytic site were not selected to avoid a reduction in enzymatic activity); and (3) amino acid residues located in loop regions that are not conserved between the thermostable β-glucosidases and MeBglD2 (Fig. 3c). Mutations III and IV correspond to rule 1 (based on amino acid alignment); mutations V and VII correspond to rule 2 (do not affect enzymatic activity); and mutations VI, VIII, and X correspond to rule 3 (non-conserved loop region).

Thermostability of MeBglD2

The mutant enzymes listed in Table S2 (Supplemental Materials) were expressed in *E. coli* and purified using nickel affinity columns, as described in the "Materials and methods." Expression of the 254P, 253GPL, and 271Tm mutants in the soluble fraction of *E. coli* was not observed (data not shown). Other mutants were expressed in the soluble fraction of *E. coli* and showed β-glucosidase activity toward *p*NP β-D-glucopyranoside (data not shown). The thermostabilities of those mutated enzymes were examined as described in "Materials and methods." Among them, the H8L, N59C, and A295G mutants exhibited much higher thermostabilities than that of the wild-type enzyme (Fig. 4a), but the thermostabilities of the other mutants, such as H8I and E118T, were not higher than that of the wild-type enzyme (data not shown). Although nearly all β-glucosidase activity of the wild-type MeBglD2 enzyme was inactivated by incubation at 56 °C for 30 min, H8L, N59C, and A295G mutants retained 13, 63, and 61% of their β-glucosidase activities, respectively, under the same conditions (Fig. 4a). Among the H8L, N59C, and A295G mutants, N59C and A295G showed much higher thermostabilities than that of H8L. The locations of these three residues within the enzyme are shown as sphere models (red: His8, Asn59, and Ala295) (Fig. 3c). Other mutation sites are indicated by different colored spheres (cyan, Glu118 and Pro210; yellow, 136-ThrPro-137 and 253-ArgTrp-254; green, 216-GNAQT-220, 271-WYGRDLVPVQPG-282, and 319-RPPGEY-324).

Next, we examined the effects of mutation combinations (H8L, N59C, and A295G) on the thermostability of MeBglD2. Double (N59C/A295G) and triple (H8L/N59C/A295G) mutants were constructed, and their thermostabilities were compared with

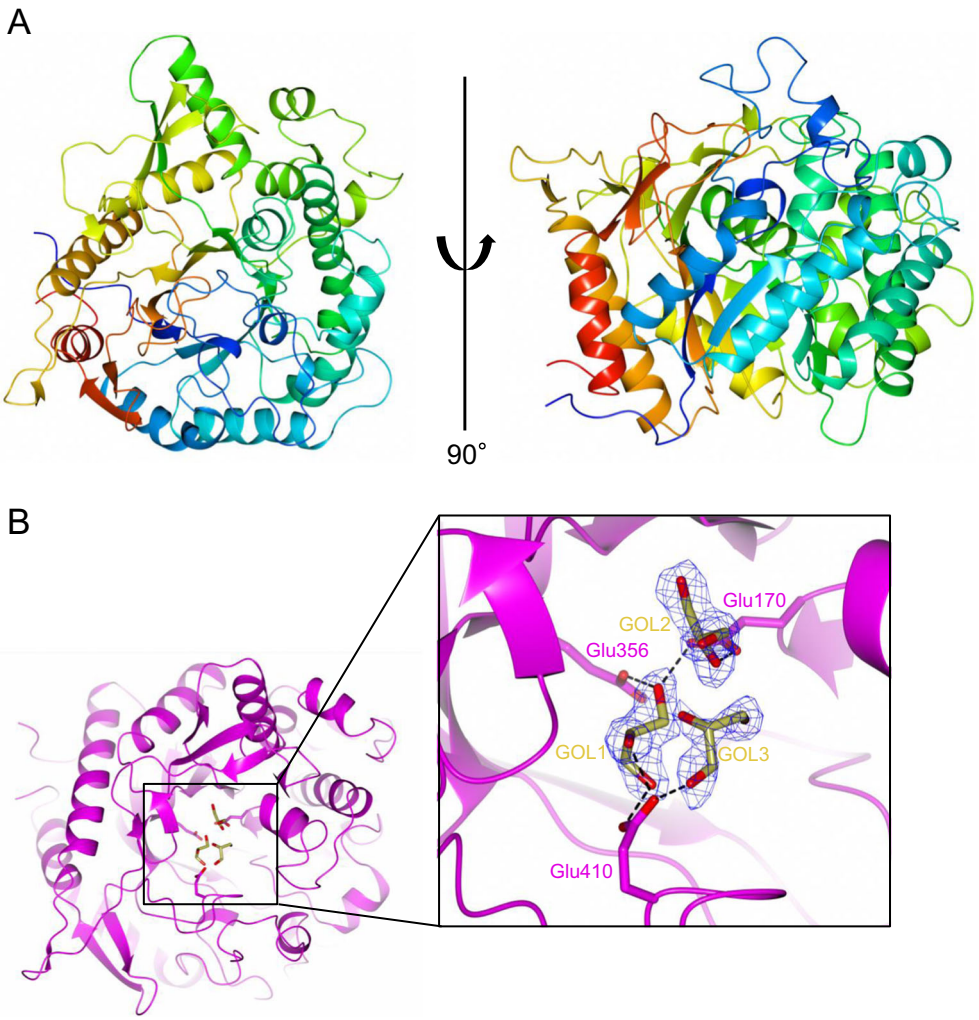

Fig. 2 Overall structure near the active site of MeBglD2. **a** The crystal structure of MeBglD2 is shown as a multi-color ribbon model. The structure consists of 11 α-helices (α1–11) and 10 β-strands (β1–10). **b** The active site of the enzyme with three glycerol molecules is shown as a magenta-colored ribbon model with a black box. The extended figure also shows three glycerol molecules (C, gold; O, red) with a density map at contoured at 1.0 σ. Hydrogen bonds among the residues (Glu170, Glu356, and Glu410) and glycerol molecules are shown as black-dashed lines

those of the wild-type and single mutants (Fig. 4a). The double (N59C/A295G) and triple (H8L/N59C/A295G) mutants retained more than 50% β-glucosidase activity after incubation at 62 °C for 30 min. The optimal temperature of the wild-type and H8L mutant enzymes was 62.5 °C. In contrast, the double (N59C/A295G) and triple (H8L/N59C/A295G) mutants exhibited the highest β-glucosidase activity at 72.5 °C (Fig. 4b). The relative activities of the double and triple mutants were similar to that of the wild-type enzyme at each optimal temperature.

The substrate specificities of the MeBglD2 mutants toward chromogenic substrates were approximately equal to that of the wild-type enzyme (see Supplemental Materials, Table S3).

Thermal shift assay of MeBglD2 mutants

The thermostability of each MeBglD2 mutant (H8L, N59C, A295G, N59C/A295G double, and H8L/N59C/A295G triple) was determined by fluorescence-based thermal shift assays using a real-time PCR detection system as described in the "Materials and methods." The T_m of each single mutant (H8L, cyan; N59C, green; A295G, yellow) was increased slightly (+ 1 ~ 3°C) relative to that of the wild-type enzyme (57.0 °C) (black in Fig. 5). However, the T_m of the double (N59C/A295G, blue) and triple (H8L/N59C/A295G, red) mutants was increased more, by + 7.0 °C (64 °C) and + 9.0 °C (66 °C), respectively (Fig. 5).

Biomass saccharification using the MeBglD2 mutants

Next, we determined whether the thermostability of MeBglD2 enhances the saccharification of cellulose biomass using a combination of *T. reesei* cellulase and MeBglD2. Wild-type MeBglD2 showed synergy with *T. reesei* cellulase and promoted biomass saccharification (Matsuzawa and Yaoi 2017). The biomass saccharification yield of the combination of *T. reesei* cellulase and MeBglD2 mutant enzymes (N59C, A295G, N59C/A295G, and H8L/N59C/A295G) was much higher than that of wild-type MeBglD2 (Fig. 6). The hydrolytic activities of the MeBglD2 mutant enzymes toward cellobiose at 40 °C were approximately equal to that of wild-type

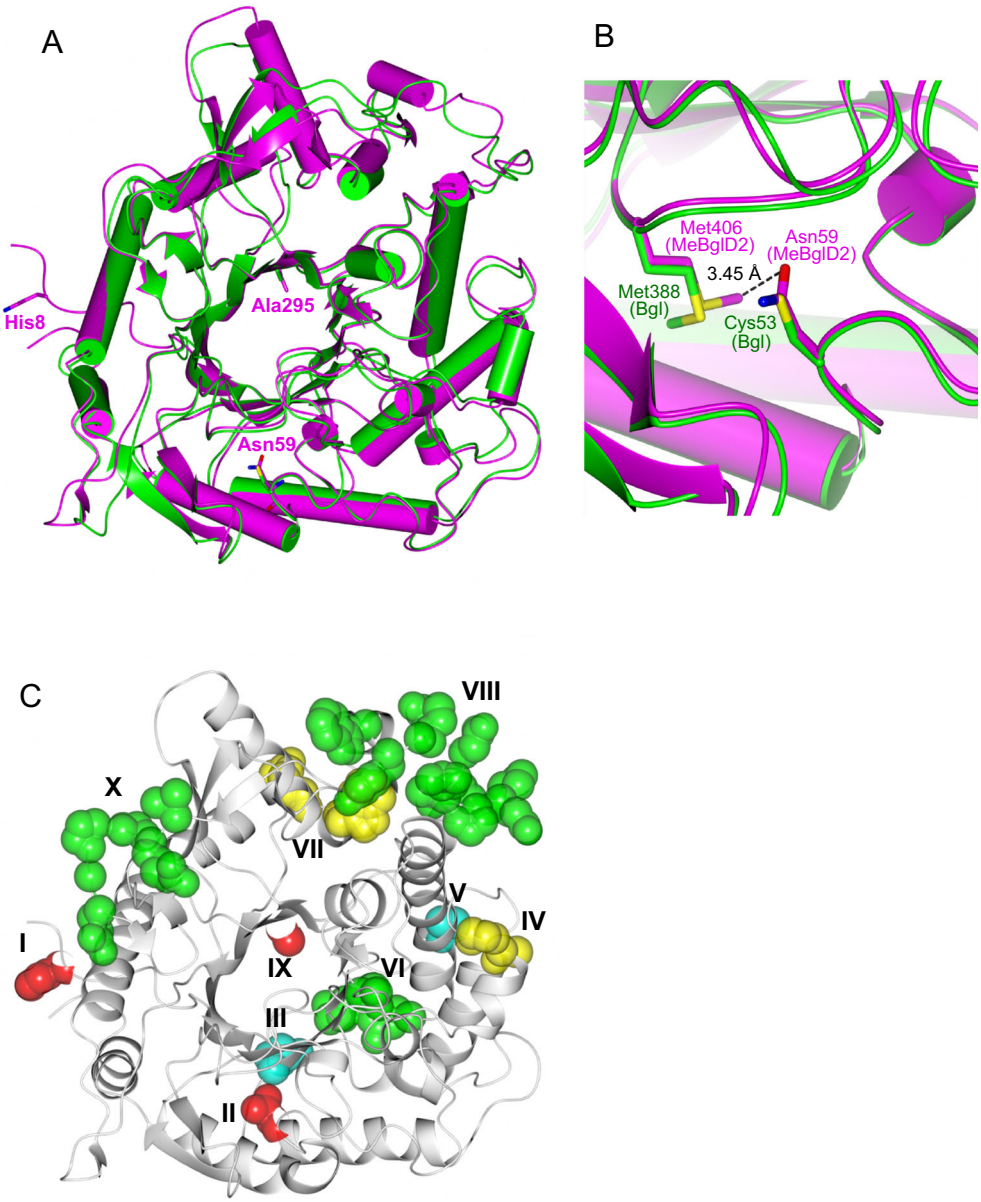

Fig. 3 Comparison of the overall structures and mutation sites of MeBglD2 and *T. thermophilus* Bgl. **a** Comparison of the overall structures of MeBglD2 (magenta) and *T. thermophilus* Bgl (green). The His8, Asn59, and Ala295 residues of MeBglD2 are shown as stick models. The Cys53 and Gly280 residues of *T. thermophilus* Bgl, corresponding to Asn59 and Ala295 of MeBglD2, respectively, are also shown as stick models. **b** The structures around the Asn59 residues of MeBglD2. MeBglD2 and *T. thermophilus* Bgl are shown in magenta and green, respectively. Asn59 and Met406 of MeBglD2 and Cys53 and Met388 of *T. thermophilus* are shown as stick models. **c** The mutation map of the enzyme is shown as a sphere model. Red: His8, Asn59, and Ala295 (Table 2, mutation sites I, II, and IX, respectively); cyan: Glu118 and Pro210 (mutation sites III and V, respectively); yellow: 136-ThrPro-137 and 253-ArgTrp-254 (mutation sites IV and VII, respectively); and green: 216-GNAQT-220, 271-WYGRDLVPVQPG-282, and 319-RPPGEY-324 (mutation sites VI, VIII, and X, respectively)

MeBglD2 (wild-type, 19.4 ± 0.2 μmol/min/mg; N59C, 18.9 ± 0.6 μmol/min/mg; A295G, 21.0 ± 2.4 μmol/min/mg; H8L/N59C/A295G, 18.8 ± 0.1 μmol/min/mg). These results indicate that the thermostability of wild-type MeBglD2 is a bottleneck for biomass saccharification, and that the thermostability of MeBglD2 enhances the saccharification yield. Although the thermostabilities of the double (N59C/A295G) and triple (H8L/N59C/A295G) mutants were much higher than that of the N59C mutant, the saccharification yields were similar.

Effects of organic solvents and copper ions

We previously reported that the hydrolytic activity of MeBglD2 was inhibited by the addition of organic solvents, ethanol, DMSO, and copper ions (Matsuzawa and Yaoi 2017). Therefore, we next examined whether mutations in H8L, N59C, and/or A295G enhance not only thermostability but also resistance to these agents (Table 2). The H8L mutant exhibited similar sensitivities toward organic solvents and copper ions as those of the wild-type enzyme. In contrast, the inhibition of β-glucosidase activity induced by organic solvents and copper ions was reduced in the H59C and A295G mutants. Although the N59C and A295G mutants exhibited similar thermostabilities, the N59C mutant showed a much higher tolerance toward organic solvents and copper ions than did the A295G mutant. The double (N59C/A295G) and triple (H8L/N59C/A295G) mutants also showed tolerance toward organic solvents and copper ions. These results indicate that mutations in N59C and A295G improve not only

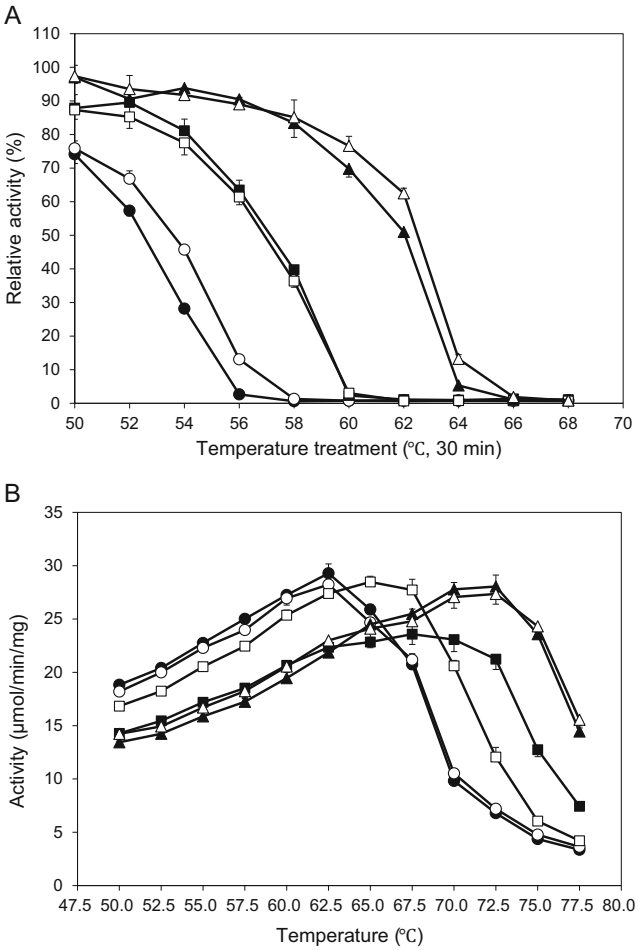

Fig. 4 Thermostabilities (**a**) and optimal temperatures (**b**) of MeBglD2 mutants. Wild-type, closed circles; H8L, open circles; N59C, closed squares; A295G, open squares; N59C/A295G, closed triangles; H8L/N59C/A295G, open triangles. Error bars: standard deviations (n = 4)

thermostability but also tolerance toward agents that inhibit the hydrolytic activity of MeBglD2. However, the mechanism

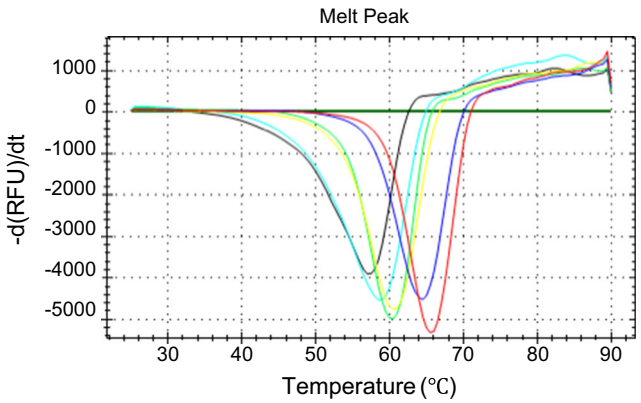

Fig. 5 Differential scanning fluorimetry experiments involving the MeBglD2 mutants. Black, wild-type; cyan, H8L; green, N59C; yellow, A295G; blue, N59C/A295G; red, H8L/N59C/A295G

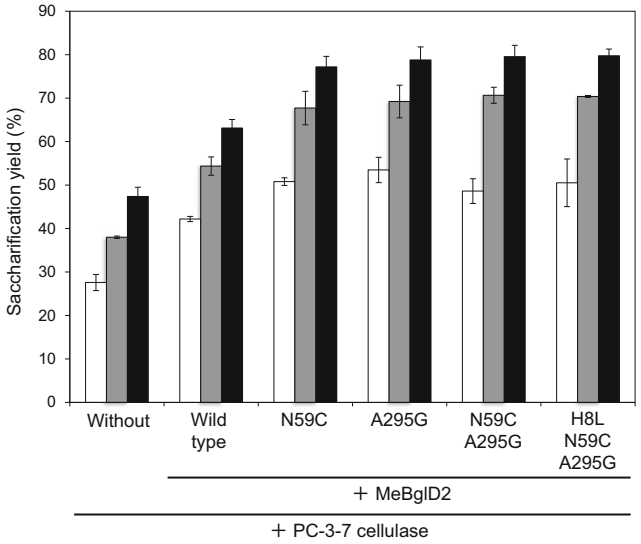

Fig. 6 Saccharification of lignocellulose biomass by a combination of *T. reesei* cellulase and MeBglD2 mutants. Alkaline-pretreated rice straw was incubated with *T. reesei* cellulase and MeBglD2 mutants at 40 °C for 24–72 h (white bars, 24 h; gray bars, 48 h; black bars, 72 h), and the concentrations of the reducing sugars released was measured. Error bars: standard deviations (n = 3)

by which ethanol and copper ions enhance the β-glucosidase activity of the N59C mutant is unclear.

Discussion

Metagenomic approaches (culture-independent genomic analyses of environmental microorganisms) are powerful tools for the isolation of new enzymes such as glycosidases (Uchiyama et al. 2015; Matsuzawa et al. 2015, 2016c; Matsuzawa and Yaoi 2017). We analyzed the crystal structure of the metagenomic β-glycosidase MeBglD2 and generated thermostable mutants using site-direct mutagenesis.

According to the Dali search, the overall structure and catalytic region of MeBglD2 resemble those of thermostable GH1 enzymes, such as *T. maritima* BglA and *T. thermophilus* Bgl. Therefore, we referred to the crystal structure and amino acid alignment of a hyperthermophilic *T. thermophilus* Bgl for improving the thermostability. In this study, we tested the thermostabilities of MeBglD2 mutants in optimal temperature and thermal shift assays. The mutations N59C and A295G were the major contributors to increased thermostability. A cysteine residue (Cys53) of the *T. thermophilus* Bgl was located at the N59 position of MeBglD2 (Fig. 1). The superimposed model between MeBglD2 and *T. thermophilus* Bgl showed that Asn59 OD1 of MeBglD2 formed a hydrogen bond with Met406 CE, and these residues almost corresponded to the locations of Cys53 and Met388 of *T. thermophilus* Bgl (Fig. 3b). We believe that the N59C mutant could be form a new hydrophobic core with

Table 2 Effects of organic solvents and copper ion toward β-glucosidase activity of MeBglD2 mutants

Relative activity (%)	No additive	10% Ethanol	10% DMSO	5 mM $CuSO_4$
Wild type	100 ± 2	20.4 ± 2.2	74.9 ± 0.9	76.1 ± 0.1
H8L	100 ± 1	25.7 ± 1.9	75.3 ± 0.4	75.0 ± 1.1
N59C	100 ± 1	119 ± 1	101 ± 2	128 ± 2
A295G	100 ± 2	57.5 ± 4.1	82.8 ± 2.4	98.7 ± 2.3
N59C/A295G	100 ± 2	127 ± 2	103 ± 3	136 ± 2
H8L/N59C/A295G	100 ± 2	129 ± 1.3	104 ± 1	136 ± 0

The β-glucosidase activities of the wild-type and mutant enzymes in the absence of these agents was defined as 100%. Error bars: standard deviations (n = 3)

Met406 in MeBglD2. Although the thermostability was 2.5–3 °C higher in A295G, the mechanism is not understood. Interestingly, the double (N59C/A295G) and triple (H8L/N59C/A295G) mutants further improved thermostability. We plan to solve the crystal structure of the mutant to elucidate the thermostability mechanism.

The thermostable MeBglD2 mutants retained their saccharide-stimulation ability (Table S3) and achieved much higher thermostability than that of the wild-type enzyme. The thermostability of MeBglD2 improved the saccharification yield of plant biomass using *T. reesei* cellulase. Several studies have reported the thermostabilities of cellulases and hemicellulases, such as cellobiohydrolases (Wu and Arnold 2013) and xylanases (Turunen et al. 2002; Xiong et al. 2004; Jun et al. 2009; Hokanson et al. 2011; Li et al. 2012, 2015; Zouari Ayadi et al. 2015; Fenel et al. 2006; Matsuzawa et al. 2016b). The inactivation of cellulose/hemicellulose-degrading enzymes is one of the most important bottlenecks for the enzymatic saccharification of plant biomass. However, other bottlenecks, including non-productive absorption of enzymes toward lignin (Várnai et al. 2011; Pribowo et al. 2012; Sørensen et al. 2013; Lou et al. 2013; Gao et al. 2014), and product inhibition (Murphy et al. 2013), are also bottlenecks for plant biomass saccharification. Our ongoing efforts will focus on overcoming these bottlenecks of the cellulose/hemicellulose-degrading enzymes.

Although the crystal structure of MeBglD2 was solved, the mechanism by which MeBglD2 is stimulated in the presence of mono- and disaccharides, such as D-glucose, D-xylose, and maltose, remains unclear. Our ongoing efforts are focused on the crystal structure of MeBglD2 in complex with *p*NP β-D-glucopyranoside/cellobiose (substrates) and D-glucose/D-xylose. The structure of MeBglD2 in complex with its substrates and additive sugars will clarify how the *p*NP β-D-glucopyranoside/*p*NP β-D-fucopyranoside degradation activity, which includes both hydrolytic and transglycosylation activities, is activated by additive sugars.

Acknowledgements The alkaline-treated rice straw was kindly provided by Dr. Yoshinori Kobayashi (Japan Bioindustry Association). The X-ray diffraction data were obtained at Beam Line BL44XU at SPring-8, Hyogo, Japan, with approval of the Institute for Protein Research, Osaka University, Osaka, Japan (proposal nos. 2016A6657 and 2016B6657).

Funding This study was funded by JSPS KAKENHI (Grant-in-Aid for Young Scientists B, Grant No. 26850067).

Compliance with ethical standards

Conflict of interest The authors declare that they have no conflict of interest.

Ethical approval This study did not involve any human participants or animals.

References

Baba Y, Sumitani JI, Tani S, Kawaguchi T (2015) Characterization of *Aspergillus aculeatus* β-glucosidase 1 accelerating cellulose hydrolysis with *Trichoderma reesei*. AMB Express 5:3

Biely P, Vrsanská M, Claeyssens M (1991) The endo-1,4-β-glucanase I from *Trichoderma reesei.* Action on β-1,4-oligomers and polymers derived from D-glucose and D-xylose. Eur J Biochem 200:157–163

Collaborative Computational Project, Number 4 (1994) The CCP4 suite: programs for protein crystallography. Acta Crystallogr Sect D: Biol Crystallogr 50:760–763

Del Pozo MV, Fernández-Arrojo L, Gil-Martinez J, Montesinos A, Chernikova TN, Nechitaylo TY, Waliszek A, Tortajada M, Rojas A, Huws SA, Golyshina OV, Newbold CJ, Polaina J, Ferrer M, Golyshin PN (2012) Microbial β-glucosidases from cow rumen metagenome enhance the saccharification of lignocellulose in combination with commercial cellulase cocktail. Biotechnol Biofuels 5:73

Dion M, Fourage L, Hallet JN, Colas B (1999) Cloning and expression of a β-glycosidase gene from *Thermus thermophilus*. Sequence and biochemical characterization of the encoded enzyme. Glycoconj J 16:27–37

Emsley P, Cowtan K (2004) Coot: model-building tools for molecular graphics. Acta Crystallogr Sect D: Biol Crystallogr 60:2126–2132

Fenel F, Zitting AJ, Kantelinen A (2006) Increased alkali stability in *Trichoderma reesei* endo-1,4-β-xylanase II by site directed mutagenesis. J Biotechnol 121:102–107

Gao D, Haarmeyer C, Balan V, Whitehead TA, Dale BE, Chundawat SP (2014) Lignin triggers irreversible cellulase loss during pretreated lignocellulosic biomass saccharification. Biotechnol Biofuels 7:175

Hokanson CA, Cappuccilli G, Odineca T, Bozic M, Behnke CA, Mendez M, Coleman WJ, Crea R (2011) Engineering highly thermostable xylanase variants using an enhanced combinatorial library methods. Protein Eng Des Sel 24:597–605

Jabbour D, Klippel B, Antranikian G (2012) A novel thermostable and glucose-tolerant β-glucosidase from *Fervidobacterium islandicum*. Appl Microbiol Biotechnol 93:1947–1956

Jun H, Bing Y, Keying Z, Xuemei D, Daiwen C (2009) Thermostable carbohydrate binding module increases the thermostability and substrate-binding capacity of *Trichoderma reesei* xylanase 2. New Biotechnol 26:53–59

Langer G, Cohen SX, Lamzin VS, Perrakis A (2008) Automated macromolecular model building for X-ray crystallography using ARP/wARP version 7. Nat Protoc 3:1171–1179

Li H, Murtomäki L, Leisola M, Turunen O (2012) The effect of thermostabilising mutations on the pressure stability of *Trichoderma reesei* GH11 xylanase. Protein Eng Des Sel 25:821–826

Li YY, Zhong KX, Hu AH, Liu DN, Chen LZ, Xu SD (2015) High-level expression and characterization of a thermostable xylanase mutant from *Trichoderma reesei* in *Pichia pastoris*. Protein Expr Purif 108:90–96

Liebl W, Gabelsberger J, Schleifer KH (1994) Comparative amino acid sequence analysis of *Thermotoga maritima* β-glucosidase BglA deduced from the nucleotide sequence of the gene indicates distant relationship between β-glucosidase of the BGA family and other families of β-1 4-glycosyl hydrolases. Mol Gen Genet 242:111–115

Lou H, Wang M, Lai H, Lin X, Zhou M, Yang D, Qiu K (2013) Reducing non-productive adsorption of cellulase and enhancing enzymatic hydrolysis of lignocelluloses by noncovalent modification of lignin with lignosulfonate. Bioresour Technol 146:478–484

Lovell SC, Davis IW, Arendall WB 3rd, de Bakker PIW, Word JM, Prisant MG, Richardson JS, Richardson DC (2003) Structure validation by Cα geometry: Φ, Ψ and Cβ deviation. Proteins 50:437–450

Matsuzawa T, Yaoi K (2017) Screening, identification, and characterization of a novel saccharide-stimulated β-glucosidase from a soil metagenomic library. Appl Microbiol Biotechnol 101:633–646

Matsuzawa T, Kaneko S, Yaoi K (2015) Screening, identification, and characterizatio of a GH43 family β-xylosidase/α-arabinofuranosidase from a compost microbial metagenome. Appl Microbiol Biotechnol 99:8943–8954

Matsuzawa T, Jo T, Uchiyama T, Manninen JA, Arakawa T, Miyazaki K, Fushinobu S, Yaoi K (2016a) Crystal structure and identification of a key amino acid for glucose tolerance, substrate specificity, and transglycosylation activity of metagenomic β-glucosidase Td2F2. FEBS J 283:2340–2353

Matsuzawa T, Kaneko S, Yaoi K (2016b) Improvement of thermostability and activity of *Trichoderma reesei* endo-xylanase Xyn III on insoluble substrates. Appl Microbiol Biotechnol 100:8043–8051

Matsuzawa T, Kimura N, Suenaga H, Yaoi K (2016c) Screening, identification, and characterization of α-xylosidase from a soil metagenome. J Biosci Bioeng 122:393–399

Matthews BW (1968) Solvent content of protein crystals. J Mol Biol 33:491–497

McCoy AJ, Grosse-Kunstieve RW, Adams PD, Winn MD, Storoni LC, Read RJ (2007) Phaser crystallographic software. J Appl Crystallogr 40:658–674

Miller GL (1959) Use of dinitrosalicylic acid reagent for determination of reducing sugar. Anal Chem 31:426–428

Murphy L, Bohlin C, Baumann MJ, Olsen SN, Sørensen TH, Anderson L, Borch K, Westh P (2013) Product inhibition of five *Hypocrea jecorina* cellulases. Enzym Microb Technol 52:163–169

Murshudov GN, Lebedev AA, Pannu NS, Steiner RA, Nicholls RA, Winn MD, Long F, Vagin AA (2011) REFMAC5 for the refinement of macromolecular crystal structures. Acta Crystallogr Sect D: Biol Crystallogr 67:355–367

Nakazawa H, Kawai T, Ida N, Shida Y, Kobayashi Y, Okada H, Tani S, Sumitani J, Kawaguchi T, Morikawa Y, Ogasawara W (2012) Construction of a recombinant *Trichoderma reesei* strain expressing *Aspergillus aculeatus* β-glucosidase 1 for efficient biomass coversion. Biotechnol Bioeng 109:92–99

Nummi M, Niku-Paavola ML, Lappalainen A, Enari TM, Raunio V (1983) Cellobiohydrolase from *Trichoderma reesei*. Biochem J 215:677–683

Otwinowski Z, Minor W (1997) Processing of X-ray diffraction data collected in oscillation mode. Methods Enzymol 276:307–326

Potterton L, McNicholas S, Krissinel E, Gruber J, Cowtan K, Emsley P, Murshudov GN, Cohen S, Perrakis A, Noble M (2004) Developments in the CCP4 molecular graphics project. Acta Crystallogr D Biol Crystallogr 60:2288–2294

Pribowo A, Arantes V, Saddler JN (2012) The absorption and enzyme activity profiles of specific *Trichoderma reesei* cellulase/xylanase components when hydrolyzing steam pretreated corn stover. Enzym Microb Technol 50:195–203

Ramani G, Meera B, Vanitha C, Rajendhran J, Gunasekaran P (2015) Molecular cloning and expression of thermostable glucose-tolerant β-glucosidase of *Penicillium funiculosum* NCL1 in *Pichia pastoris* and its characterization. J Ind Microbiol Biotechnol 42:553–565

Saloheimo M, Lehtovaara P, Penttilä M, Teeri TT, Ståhlberg J, Johansson G, Pettersson G, Claeyssens M, Tomme P, Knowles JK (1988) EGIII, a new endoglucanase from *Trichoderma reesei*: the characterization of both gene and enzyme. Gene 63:11–22

Senisterra GA, Finerty PJ Jr (2009) High throughput methods of assessing protein stability and aggregation. Mol BioSyst 5:217–223

Sørensen A, Lübeck M, Lübeck PS, Ahring BK (2013) Fungal β-glucosidases: a bottleneck in industrial use of lignocellulosic materials. Biomol Ther 3:612–631

Teeri TT, Koivula A, Linder M, Wohlfahrt G, Divne C, Jones TA (1998) *Trichoderma reesei* cellobiohydrolases: why so efficient on crystalline cellulose? Biochem Soc Trans 26:173–178

Teugjas H, Väljamäe P (2013) Selecting β-glucosidases to support cellulases in cellulose saccharification. Biotechnol Biofuels 6:105

Teze D, Hendrickx J, Czjzek M, Ropartz D, Sanejouand YH, Tran V, Tellier C, Dion M (2014) Semi-rational approach for converting a GH1 β-glycosidase into a β-transglycosidase. Protein Eng Des Sel 27:13–19

Turunen O, Vuorio M, Fenel F, Leisola M (2002) Engineering of multiple arginines into Ser/Thr surface of *Trichoderma reesei* endo-1,4-β-xylanase II increases the thermotolerance and shifts the pH optimum towards alkaline pH. Protein Eng 15:141–145

Uchima CA, Tokuda G, Watanabe H, Kitamoto K, Arioka M (2012) Heterologous expression in *Pichia pastoris* and characterization of an endogenous thermostable and high-glucose-tolerant β-glucosidase from the termite *Nasutitermes takasagoensis*. Appl Environ Microbiol 78:4288–4293

Uchiyama T, Miyazaki K, Yaoi K (2013) Characterization of a novel β-glucosidase from a compost microbial metagenome with strong transglycosylation activity. J Biol Chem 288:18325–18334

Uchiyama T, Yaoi K, Miyazaki K (2015) Glucose-tolerant β-glucosidase retrieved from a Kusaya gravy metagenome. Front Microbiol 5:548

Várnai A, Viikari L, Marjamaa K, Siika-aho M (2011) Adsorption of monocomponent enzymes in enzyme mixture analyzed quantitatively during hydrolysis of lignocellulose substrates. Bioresour Technol 102:1220–1227

Watanabe M, Inoue H, Inoue B, Yoshimi M, Fujii T, Ishikawa K (2014) Xylanase (GH11) from *Acremonium cellulolyticus*: homologous expression and characterization. AMB Express 4:27

Wu I, Arnold FH (2013) Engineered thermostable fungal Cel6A and Cel7A cellobiohydrolases hydrolyze cellulose efficiently at elevated temperatures. Biotechnol Bioeng 110:1874–1883

Xiao Z, Zhang X, Gregg DJ, Saddler JN (2004) Effects of sugar inhibition on cellulases and β-glucosidase during enzymatic hydrolysis of softwood substrates. Appl Biochem Biotechnol 115:1115–1126

Xiong H, Fenel F, Leisola M, Turunen O (2004) Engineering the thermostability of *Trichoderma reesei* endo-1,4-β-xylanase II by combination of disulphide binding. Extremophiles 8:393–400

Yang F, Yang X, Li Z, Du C, Wang J, Li S (2015) Overexpression and characterization of a glucose-tolerant β-glucosidase from *T. aotearoense* with high specific activity for cellobiose. Appl Microbiol Biotechnol 99:8903–8915

Yernool DA, McCarthy JK, Eveleigh DE, Bok JD (2000) Cloning and characterization of the glucooligosaccharide catabolic pathway beta-glucan glucohydrolase and cellobiose phosphorylase in the marine hyperthermophile *Thermotoga neapolitana*. J Bacteriol 182:5172–5179

Zechel DL, Boraston AB, Gloster T, Boraston CM, Macdonald JM, Tilbrook DM, Stick RV, Davies GJ (2003) Iminosugar glycosidase inhibitors: structural and thermodynamic dissection of the binding of isofagomine and 1-deoxynojirimycin to β-glucosidases. J Am Chem Soc 125:14313–14323

Zouari Ayadi D, Hmida Sayari A, Ben Mabrouk S, Mezghani M, Bejar S (2015) Improvement of *Trichoderma reesei* xylanase II thermal stability by serine to threonine surface mutations. Int J Biol Macromol 72:163–170